J Polym Res (2013) 20:32
DOI 10.1007/s10965-012-0032-1

ORIGINAL PAPER

Properties of poly(vinylidene fluoride)-graft-poly (*N*-isopropylacrylamide) membranes prepared by alkali treatment

Yiping Zhao · Jingna Bai · Xia Feng · Li Chen · Xiang Shen · Meijun Liu · Jianxin Li

Received: 23 June 2012 / Accepted: 15 November 2012 / Published online: 15 January 2013
© Springer Science+Business Media Dordrecht 2013

Abstract An amphiphilic graft copolymer (PVDF-g-PNIPAAm) with poly(vinylidene fluoride) (PVDF) main chains and poly(N-isopropylacrylamide) (PNIPAAm) side chains was synthesized via radical copolymerization, and flat sheet membranes of this copolymer were prepared by the phase inversion method. The process of membrane formation was investigated by ultrasonic time-domain reflectometry (UTDR). The structures and properties of the membrane, including its surface chemical structure, pore morphology, and water permeability, were characterized by X-ray photoelectron spectroscopy (XPS), scanning electron microscopy (SEM), and a water permeation experiment, respectively. The relationship between the process of membrane formation and the properties of the membrane was studied. The results showed that the membrane displayed temperature sensitivity. Treating the PVDF for a longer period with alkali caused more PNIPAAm to graft onto the main chains, which influenced not only the microporous structure and formation process of the membrane but also the temperature sensitivity of the performance of the membrane.

Keywords PVDF-g-PNIPAAm · Ultrasonic time-domain reflectometry (UTDR) · Temperature-sensitive · Membrane

Y. Zhao (✉) · J. Bai · X. Feng · L. Chen (✉) · X. Shen · M. Liu · J. Li
School of Material Science & Engineering, Tianjin Polytechnic University, Tianjin 300387, People's Republic of China
e-mail: yipingzhao@sina.com
e-mail: tjpuchenlis@163.com

Y. Zhao · L. Chen · J. Li
The Key Laboratory of Hollow Fiber Membrane Material and Membrane Process of the Ministry of Education, Tianjin 300387, People's Republic of China

Introduction

During the past few decades, more and more technical fields have begun to focus on stimulus-responsive polymers and membranes that exhibit distinct but predictable changes in properties in response to the alterations in pH, temperature, electric field, or the addition of chemicals [1–6]. Poly(*N*-isopropylacrylamide) (PNIPAAm) is a typical temperature-sensitive polymer with a lower critical solution temperature (LCST) of around 32 °C. Below the LCST, the PNIPAAm polymer chains assume an extended random coil conformation in water; above the LCST, the polymer chains dehydrate to form a compact structure [7, 8]. PNIPAAm can be used to prepare temperature-sensitive PVDF membranes for various applications by grafting PNIPAAm onto the existing membrane or PVDF powder [9, 10]. Such membranes show temperature-sensitive performance and possess the desirable properties of the PVDF matrix. The former study shows that the temperature-dependent behavior of a PVDF-g-PNIPAAm membrane is closely related to its grafting ratio and the arrangement of PNIPAAm in the PVDF-g-PNIPAAm membrane [10].

We have reported the graft copolymerization of PNIPAAm onto a PVDF hollow-fiber membrane using an alkali treatment and the subsequent synthesis of the PVDF-g-PNIPAAm copolymer [11, 12]. In the present work, the grafting ratio of PNIPAAm was adjusted by varying the alkali treatment time to elucidate the relationship between the grafting ratio of PNIPAAm and the structures and properties of the corresponding membranes. The process of PVDF-g-PNIPAAm membrane formation was investigated systematically by ultrasonic time-domain reflectometry (UTDR). UTDR is a versatile measurement technique that is extensively used to monitor fouling and cleaning processes in different membrane module configurations, such as flat-sheet, tubular, and hollow-fiber membranes [13, 14]. It was developed to characterize thickness changes during evaporative casting and solidification phenomena in

membrane systems [15]. In this work, the membrane formation process was monitored in real time using UTDR. The results of our experiments will hopefully be useful for preparing PVDF-g-PNIPAAm membranes for various applications.

Experimental

Materials

N-isopropylacrylamide (NIPAAm, 95 %), used after further purification, was purchased from Kohjin Co., Ltd. (Tokyo, Japan). Poly(vinylidene fluoride) (PVDF Solef 1010) was obtained from Solvey Co., Ltd. (Brussels, Belgium). 2,2′-Azobisisobutyronitrile (AIBN, 99 %) was provided by Shanghai Shisihewei Chemical Co., Ltd. (Shanghai, China), and was recrystallized from ethanol before use. *N*,*N*-dimethylformamide (DMF) was supplied by Kemiou Chemical Co., Ltd. (Tianjin, China). All other reagents were of analytical grade and were used as received.

Synthesis of PNIPAAm-based temperature-sensitive copolymers

A detailed summary of the method used to synthesize the PVDF-g-PNIPAAm copolymers was provided in a previous work [11]. PVDF pellets were immersed in a 10 wt% KOH solution containing 0.05 wt% ethanol, and the solution was then stirred at 60 °C. The alkali treatment was applied for either 4, 7, 13, or 16 min, respectively. After the solution had cooled, the precipitate was collected by filtration and washed four times with distilled water to remove the alkali solution. The alkali-treated PVDF powder was then dissolved in DMF at 60 °C. Subsequently, NIPAAm and AIBN were added to the solution in order to prompt graft polymerization. Under nitrogen protection and vigorous stirring, the reaction was carried out at 60 °C for 10 h. The reaction solution was precipitated by methanol and collected by filtration. To remove NIPAAm monomer residue, the raw product was washed with distilled water. The product was dried fully in a vacuum oven at 40 °C before further characterization and membrane preparation. The grafting ratio of the PVDF-g-PNIPAAm copolymer was confirmed by ^{1}H NMR performed using an AVANCE 300 MHz instrument from Bruker (Bremen, Germany). The number average molecular weight (M_n) of the PVDF-g-PNIPAAm copolymer was measured using a quaternary pump HPLC system (model 1200, Agilent, Santa Clara, CA, USA) equipped with differential refractive index detector (RID).

Preparation of temperature-sensitive membranes

Each PVDF-g-PNIPAAm membrane was prepared via the conventional phase inversion method [16, 17]. In a representative procedure, a casting solution was prepared by fully dissolving the polymers in DMF with a weight fraction of the polymer of 15 wt%. The solution was stirred for 2 h at 60 °C and then left for 6 h to allow all of the air bubbles to dissipate. After cooling to room temperature, the casting solution was dispersed uniformly on a glass plate and cast by a knife to a thickness of 0.2 mm. The nascent membrane was immersed immediately in distilled water to induce the formation of the PVDF-g-PNIPAAm membrane. The membranes obtained using this technique (named M4, M7, M13, and M16 respectively, according to the alkali treatment time) were thoroughly rinsed with distilled water to remove the residual solvent and soaked in water before use.

Characterization of the temperature-sensitive membranes

The chemical compositions of the surfaces of the prepared membranes were analyzed by X-ray photoelectron spectroscopy (XPS, Genesis 60S, EDAX Inc., Mahwah, NJ, USA). The morphologies of the surfaces and cross-sections of the membranes were inspected by scanning electron microscopy (SEM, s-4800, Hitachi, Tokyo, Japan). The membranes were fractured in liquid nitrogen to obtain a tidy cross-section, and then sputter-coated with gold and visualized by SEM.

Monitoring the membrane formation process by UTDR

Ultrasonic time-domain reflectometry (UTDR) was employed as a visualization technique to provide real-time monitoring of the PVDF-g-PNIPAAm membrane formation process. The ultrasonic measurement system employed was reported in a previous paper [18]. The casting solution was dispersed uniformly on a glass plate and placed between two polymethyl methacrylate (Perspex) plates, and the cell was then immersed in a coagulation bath at 25 °C while monitoring the ultrasonic signal. The signal from a blank sample without casting solution on the glass plate was collected in advance and considered to be the approximate initial ultrasonic signal from the membrane formation process.

The transducer was used as not only a transmitter but also a receiver. The ultrasonic wave pulses transmitted by the transducer propagated through the coagulation bath, casting solution, and then glass plate. When an ultrasonic wave encounters an interface between two media (e.g., the coagulation bath/casting solution interface and the casting solution/glass plate interface), energy will generally be partitioned such that a reflected wave occurs. The arrival time required for ultrasonic waves to return the transducer (Δt) can be obtained [19]. As per the theory described in a previous work [20], the membrane formation process can be investigated and the speed of membrane formation can be measured.

Permeation experiments

The water flux through the membranes was measured using a home-made filtration apparatus. The effective area of the tested membranes was 12.56 cm^2. The membrane was pre-pressurized under a pressure of 0.1 MPa for 1 h before test. During the measurements, the test cell and permeating solution were kept at a given temperature. The pure water flux was calculated as follows:

$$J = \frac{V}{At}, \tag{1}$$

where J is the flux (L/m^2h), V is the permeate volume (L), A is the effective membrane area (m^2), and t represents the time (h), respectively.

The flux ratio (FR) was introduced to reflect the temperature-dependent permeation of the membrane. It was calculated as follows:

$$FR = \frac{J_{37}}{J_{22}} \times 100\%, \tag{2}$$

where J_{37} is the flux (L/m^2h) at 37 °C and J_{22} is the flux (L/m^2h) at 22 °C.

Results and discussion

Characterization of PVDF-g-PNIPAAm copolymers

Figure 1 shows ^1H NMR spectra of PVDF and PVDF-g-PNIPAAm copolymers. The peaks at 3.32 and 2.90 ppm are due to head-to-tail (ht, $CH_2CF_2CH_2CF_2$) and head-to-head (hh, $CF_2CH_2CH_2CF_2$) bonding arrangements of PVDF. In comparison with the spectrum of PVDF, the grafting of PNIPAAm to PVDF results in the appearance of a peak in the region of 1.0–1.1 ppm, which can be attributed to the methyl proton of the isopropyl group ($CH(CH_3)_2$). This indicates that NIPAAm has been successfully grafted onto the main chain of the alkali-treated PVDF. The grafting ratio of NIPAAm in the PVDF-g-PNIPAAm copolymer, M_c, is defined as follows:

$$M_c = \frac{\frac{1}{6}A}{\frac{1}{2}(A_{ht} + A_{hh}) + \frac{1}{6}A} \times 100\%, \tag{3}$$

where A is the area of the absorption peak due to ($(CH_3)_2CH$), whereas A_{ht} and A_{hh} are the areas of the absorption peaks due to PVDF (ht) and PVDF (hh).

After alkali treatment, the PVDF chains contain C=C double bonds and are active radicals in the reaction system. Generally, more C=C double bonds are produced as the the alkali treatment period is extended. Thus, increasing the treatment time leads to more active radicals, which in turn causes more of the NIPAAm chains to be grafted onto the main chains. The M_c and M_n values of the PVDF-g-PNIPAAm copolymers both increased with increasing alkali treatment time, as shown in Table 1.

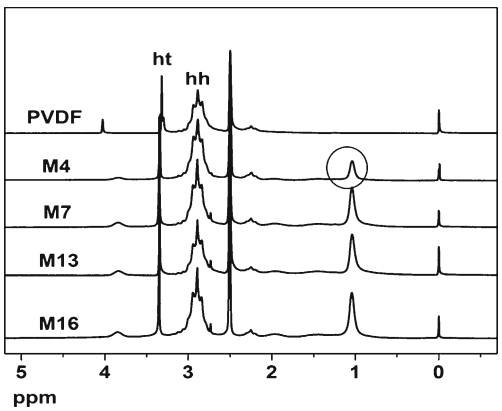

Fig. 1 ^1H NMR spectra for the PVDF and the PVDF-g-PNIPAAm copolymers prepared by treatment with alkali for different periods

Monitoring the membrane formation process

Figure 2 shows ultrasonic signal spectra obtained during the PVDF-g-PNIPAAm membrane formation process. The line labeled "glass" is the ultrasonic signal from the blank sample without casting solution, which was considered to be the initial signal during the membrane formation process. The lines labeled 5 s, 10 s, 12 s, and so on are the ultrasonic signals obtained at different membrane formation times.

Changes in the arrival times (Δt) of ultrasonic signals imply changes in the density of the media through which the ultrasonic signals pass through. As the viscous solution changes into a gel and then into a porous membrane, the density of the casting solution increases and the ultrasonic signals gradually shift forward [21]. In Fig. 2a (M4), the arrival times of the ultrasonic signals continuously decrease, which indicates that the density of the medium increases. However, the arrival times for the spectra obtained at formation times of 12 s and 15 s are very similar, which means that the density of the casting solution does not change notably beyond 12 s. Therefore, this formation time (12 s) was regarded as the membrane solidification time.

Table 1 M_c and M_n values of PVDF-g-PNIPAAm copolymers treated for different periods with alkali

Membrane	M_c (%)	M_n ($\times 10^4$)
M4	6.28	6.49
M7	11.65	7.51
M13	11.89	7.75
M16	12.13	8.11

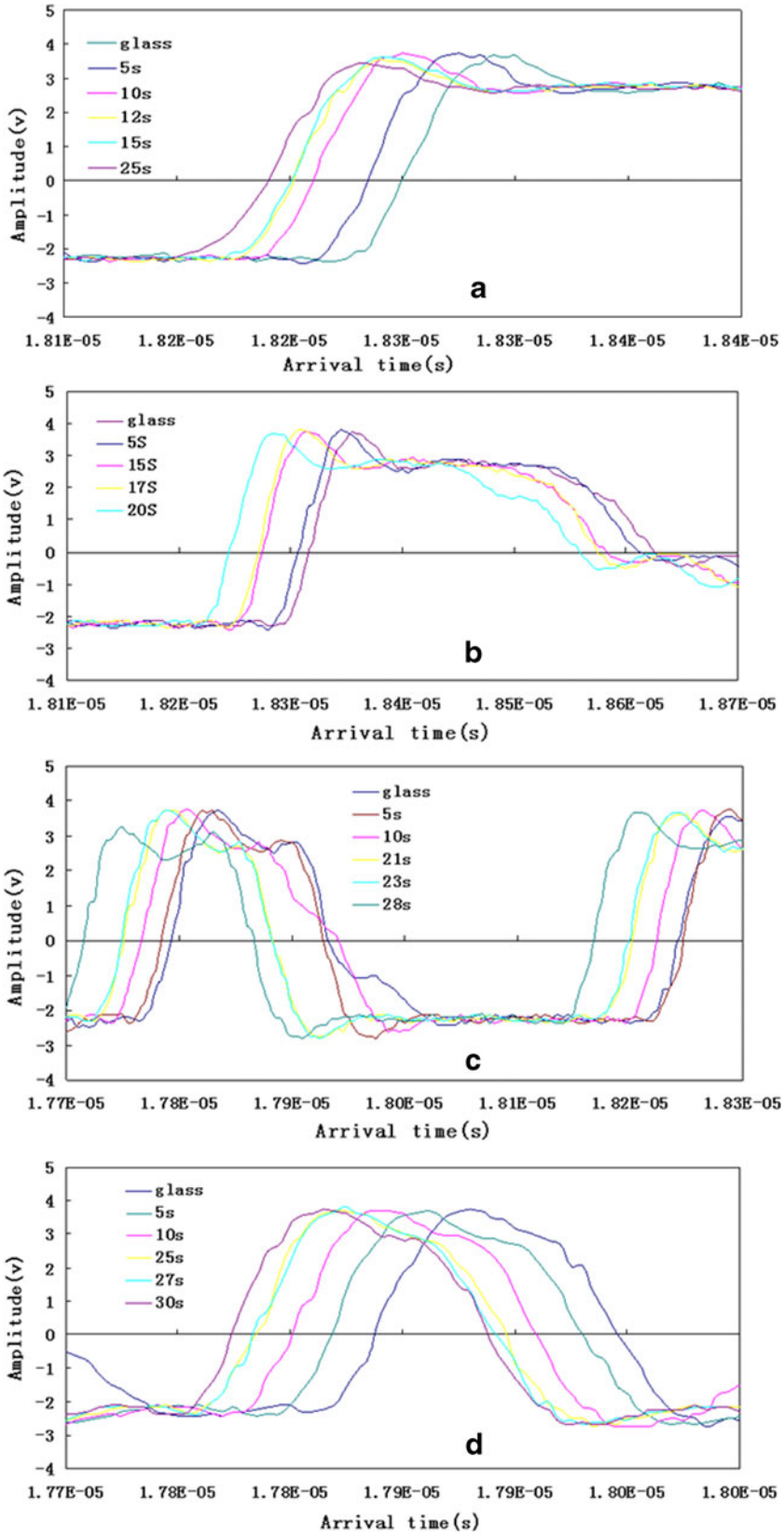

Fig. 2 a–d Ultrasonic signal spectra obtained during the formation of the following PVDF-g-PNIPAAm membranes: **a** M4, **b** M7, **c** M13, **d** M16

Based on the analysis provided above, the membrane solidification times of M7, M13, and M16 were found to be 15, 21, and 25 s, respectively. These results demonstrate that the membrane solidification time increases with increasing alkali treatment time. As the PNIPAAm content is increased, the hydration of the casting solution and water

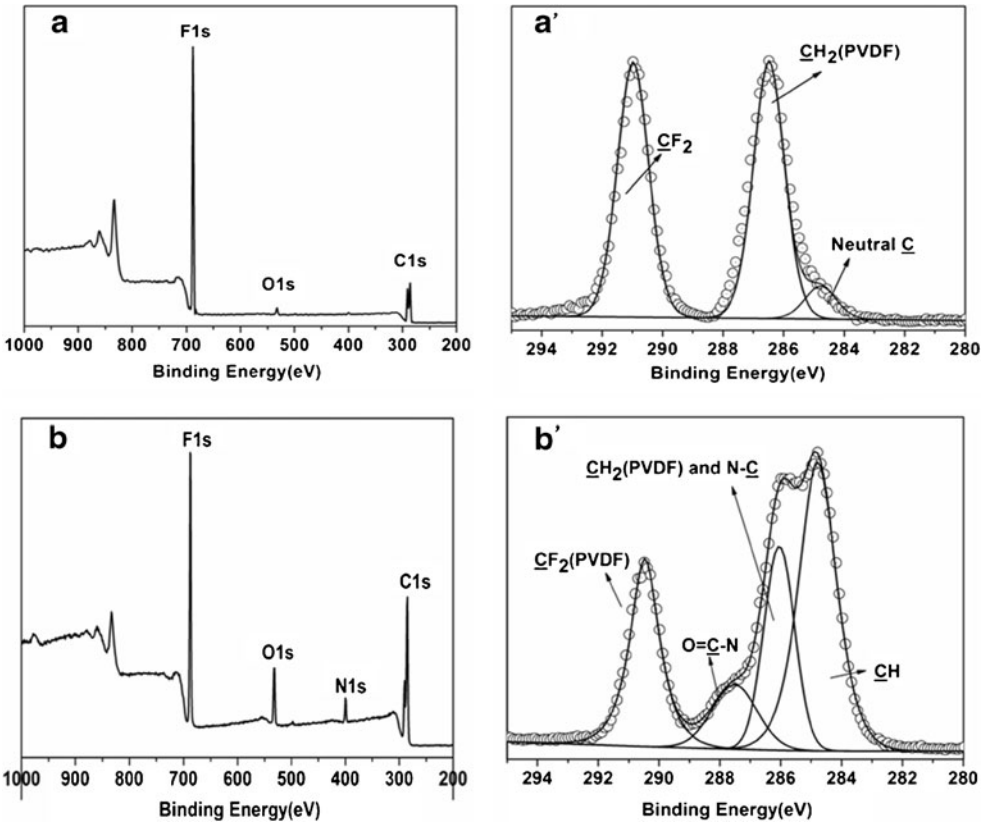

Fig. 3 a–b XPS wide-scan spectra of the PVDF and M4 membranes: **a**, **a′** PVDF; **b**, **b′** M4

increase, which means that the tolerance of the casting solution to non-solvent molecules improves, decreasing the exchange diffusion between solvent and non-solvent [11].

Surface compositions of the copolymer membranes

Figure 3 presents wide scans and C1*s* core-level spectra for the PVDF and M4 membrane. For the pristine PVDF membrane (Fig. 3a), the wide-scan spectra showed peaks from C1*s*, F1*s*, and O1*s*. The peak due to O1*s* is present due to air pollution. In the wide-scan spectrum of the PVDF-g-PNIPAAm membrane (Fig. 3b, b′), a signal from N1*s* occurs at a binding energy (BE) of about 398.5 eV, which is from the grafted PNIPAAm. For the pristine PVDF membrane, the C1*s* core-level spectrum can be curve-fitted with three peak components at binding energies (BEs) of 290.7 eV (for the $\underline{C}F_2$ group), 286.2 eV (for the $\underline{C}H_2$ group), and 284.8 eV (for the neutral $\underline{C}H$ group). The ratio of the $\underline{C}F_2$ to the $\underline{C}H_2$ peak components is about 1, which is in good agreement with the chemical stoichiometry of PVDF. On the other hand, for the PVDF-g-PNIPAAm membrane, an additional peak component is present at a BE of 287.8 eV, which can be assigned to O=$\underline{C}$–N groups in the grafted PNIPAAm. The N–$\underline{C}$ (PNIPAAm) peak component, which has the same BE as that of $\underline{C}H_2$ (PVDF), is present at a BE of 286.2 eV. The $\underline{C}H$ (PNIPAAm) component with a BE of 284.8 eV can be assigned to the hydrocarbon backbone of the PNIPAAm. The two peaks at 286.2 eV and 290.7 eV are attributable to the $\underline{C}H_2$ and $\underline{C}F_2$ groups in the PVDF main chains, respectively. The core-level spectral area ratios of various C1*s* peaks from the surfaces of PVDF-g-PNIPAAm membranes are shown in Table 2.

Table 2 Core-level spectral area ratios of various C1*s* peaks from the surfaces of PVDF-g-PNIPAAm membranes

Membrane	$\underline{C}H$ (%)	N–$\underline{C}$ and $\underline{C}H_2$(PVDF) (%)	O=$\underline{C}$–N (%)	$\underline{C}F_2$ (PVDF) (%)
M4	42.24	25.76	10.83	21.17
M7	47.67	19.36	11.23	21.74
M13	42.41	24.24	11.41	21.94
M16	54.64	18.03	13.90	13.42

Table 3 Mole fractions of NIPAAm in the PVDF-g-PNIPAAm bulk copolymer and in the membrane surface

Membrane	Mole fraction of NIPAAm (%)	
	Membrane surface (measured via XPS)	Copolymer bulk (measured via ^{1}H NMR)
M4	33.84	15.26
M6	34.06	23.62
M13	34.21	29.82
M16	50.88	20.34

The mole fraction (M_s) of NIPAAm in the surface of a PVDF-g-PNIPAAm membrane is readily calculated using

$$M_s = \frac{A_{(N-C=O)}}{A_{(N-C=O)} + A_{CF_2}} \times 100\%, \quad (4)$$

where $A_{(N-C=O)}$ is the intensity of the O=C–N peak and A_{CF2} is the intensity of the CF_2 peak.

The results are listed in Table 3. For each PVDF-g-PNIPAAm copolymer, the M_s value (determined by ^{1}H NMR analysis) is much higher than the M_c value. This phenomenon is due to the enrichment of the PNIPAAm

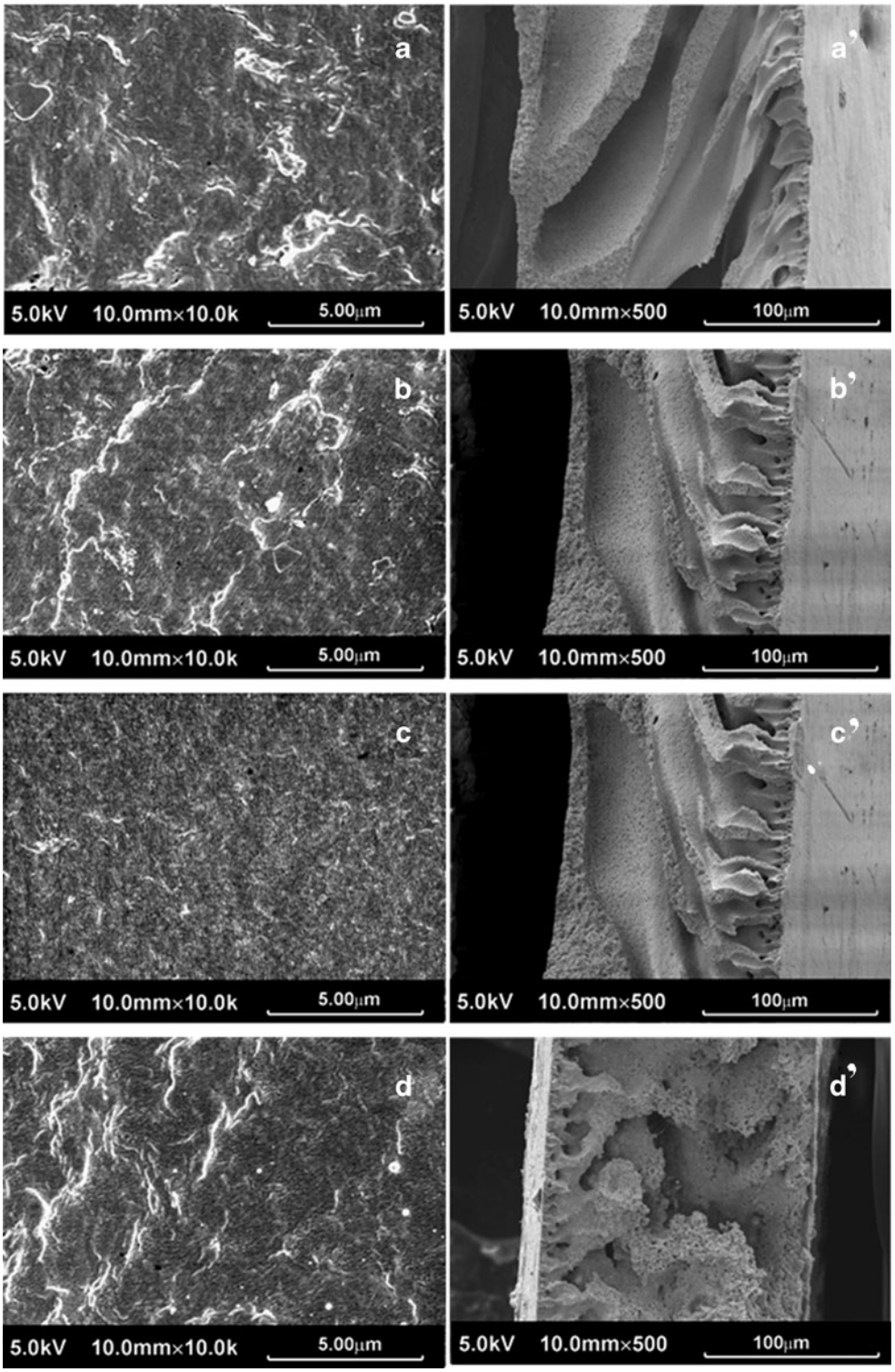

Fig. 4 a–d Surface and cross-sectional morphologies of PVDF-g-PNIPAAm membranes: **a**, **a′** M4; **b**, **b′** M7; **c**, **c′** M13; **d**, **d′** M16

polymer at the outermost surface during membrane formation in the aqueous medium. The copolymer possesses an amphiphilic structure with hydrophobic PVDF chains and hydrophilic PNIPAAm chains below its LCST. When pure water at 25 °C is used as the coagulation bath, PNIPAAm prefers to move into the water coagulation bath. Also, the M_s value of the PVDF-g-PNIPAAm membrane increases with increasing membrane formation time, because a fair amount of tine is needed for the enrichment of PNIPAAm to occur at the interface. Therefore, the PNIPAAm content in the membrane surface is higher than it is in the bulk copolymer.

Membrane morphology

The surface and cross-sectional morphologies of PVDF-g-PNIPAAm membranes with different alkali treatment times are shown in Fig. 4. Figure 4 depicts the surface morphologies of PVDF-g-PNIPAAm membranes, as observed by SEM. This result is in good agreement with the results of the previous investigation reported by Kang [22], who introduced the pore-forming mechanism of PNIPAAm. In the membrane formation process, the hydrophobic PVDF chains gradually shrink while the PNIPAAm chains remain fully extended in the coagulation bath. The copolymer displays an irregularly micelle-like aggregation process. Strong repulsion arising from the incompatibility of the PVDF main chains with the PNIPAAm side chains forces the copolymers to undergo partial phase separation in the aqueous medium. First, the PVDF main chains precipitate from the casting solution system. Meanwhile, the hydrophilic PNIPAAm side chains form a hydrous layer on the membrane surface. After drying, the PNIPAAm chains bend down onto the hydrophobic PVDF chains, facilitating the formation of well-defined microporous structures [23, 24].

The surface porosity of the membrane is found to increase with increasing grafting ratio of PNIPAAm. Similar results have been obtained in previously published studies [22, 25–27]. This may be attributed to the occurrence of irregularly micelle-like aggregation during membrane casting by phase inversion. Increasing the grafting ratio of PNIPAAm results in a copolymer with a greatly enhanced hydrophilic side-chain density, which contributes to an increase in the amount of micelle-like aggregation and thus the formation of a membrane surface with much greater microporosity.

Figure 4 also displays the cross-sectional morphologies of the PVDF-g-PNIPAAm membranes. Finger-like macrovoids are observed in these cross-sections. This indicates that the phase separation of the PVDF-g-PNIPAAm copolymer is determined by instantaneous liquid–liquid phase separation due to fast exchange diffusion between the solvent and non-solvent. This is in accord with the results of UTDR.

Pure water permeation properties

The pure water fluxes at 22 °C and 37 °C of the membranes were measured in permeation experiments. Temperature-dependent fluxes through the copolymer membranes were characterized by the flux ratio (FR, J_{37}/J_{22}). As shown in Fig. 5, the fluxes of all of the membranes at 37 °C were higher than they were at 22 °C (FR>1). The reason for this is that the viscosity of water is lower at 37 °C than at 22 °C. The FR values of the copolymer membranes are higher than that of the PVDF membrane when the alkali treatment time exceeds 7 min. This behavior can be explained by a valve mechanism resulting from the transition between polymer expansion below the LCST of PNIPAAm and the shrinkage above the LCST. At the permeation temperature below the LCST, the PNIPAAm-grafted chains exhibit an extended random coil conformation. On the other hand, PNIPAAm-grafted chains shrink due to the dehydration at the temperature above the LCST, leading to a release of the clogging of membrane pore, the pore size increased and the membrane showed a dramatic increase of water flux.

When the alkali treatment time exceeds 7 min, the FR values of the copolymer membranes are similar. That is, the temperature sensitivities of the PVDF-g-PNIPAAm membranes are similar; there is no significant relation to the PNIPAAm grafting ratio. From Figs. 4 and 5, it is also difficult to discern a clear relationship between the temperature sensitivity and the membrane morphology. The temperature sensitivity of the flux through the membranes is known to be influenced by the pore size, pore size distribution, the PNIPAAm grafting ratio, the PNIPAAm content of the pore surface, the length of PNIPAAm chains, and so on. It is impossible to confirm a relationship between membrane morphology and temperature sensitivity. Similarly, it is impossible to confirm a relationship between the grafting yield of PNIPAAm and temperature sensitivity. In addition, the grafting yield of PNIPAAm also influences both the membrane formation process (Fig. 2) and the membrane morphology (Fig. 4). We therefore need to study this complex web of interrelations further in our future work.

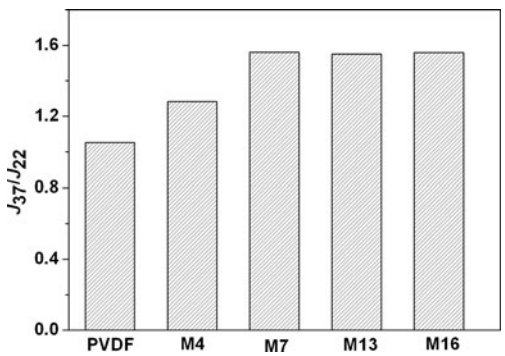

Fig. 5 Influence of temperature on the water fluxes of PVDF-g-PNIPAAm membranes with different alkali treatment times

Conclusions

PVDF-g-PNIPAAm membranes with different grafting ratios of PNIPAAm were successfully prepared via the phase inversion method. Increasing the alkali treatment time of PVDF led to a higher grafting ratio of PNIPAAm, which prolonged the membrane solidification time. Due to the surface segregation of PNIPAAm chains during the membrane formation process, the PNIPAAm concentration on the membrane surface was higher than that in the PVDF-g-PNIPAAm copolymer. Because of the pore-forming ability of PNIPAAm, far more microporous structures are formed on the membrane surface when the grafting ratio of PNIPAAm is increased, which facilitates the production of membranes with useful temperature sensitive properties.

Acknowledgements This work was financially supported by the National Science Foundation of China (grant numbers 21074091, 21174103, and 31200719), the Project for Science and Technical Development of China (grant number 2007AA03Z533), the Science Foundation of Tianjin (grant number 12JCYBJC11200), and the Key Grant Project of the Chinese Ministry of Education (grant number 209005).

References

1. Roh DK, Ahn SH, Seo JA, Shul YG, Kim JH (2010) J Polymer Sci B Polymer Phys 48:1110–1117
2. Klaikherd A, Nagamani C, Thayumanavan S (2009) J Am Chem Soc 131:4830–4838
3. Wanderaa D, Wickramasingheb SR, Hussona SM (2010) J Am Chem Soc 357:6–35
4. Bittrich E, Kuntzsch M, Eichhorn KJ, Uhlmann P (2010) J Polymer Sci B Polymer Phys 48:1606–1615
5. Iwata H, Matsuda T (1988) J Membr Sci 38:185–199
6. Hirata I, Okazaki M, Iwata H (2004) Polymer 45:5569–5578
7. Zhang J, Chu LY, Cheng CJ, Mi DF, Zhou MY, Ju XJ (2008) Polymer 49:2595–2603
8. Cheng JG, Wang L, Huo J, Yu HJ, Yang Q, Deng LB (2008) J Polymer Sci B Polymer Phys 46:1529–1535
9. Ying L, Kang ET, Neoh KG (2002) Langmuir 18:6416–6423
10. Neoh JZ, Zhu LP, Zhu BK, Xu YY (2011) J Membr Sci 366:176–183
11. Guo YF, Feng X, Chen L, Zhao YP, Bai JN (2010) J Appl Polym Sci 116:1005–1009
12. Wang WY, Chen L, Yu X (2006) J Appl Polym Sci 101:833–837
13. Sanderson RD, Li JX, Hallbauer DK (2005) Environ Sci Technol 39:7299–7305
14. Anim-Mensah AR, Franklin JE, Palsule AS, Salazar LA, Widenhouse CW, Mast DB, Mark JE, Krantz WB, Clarson SJ (2010) ACS Symp Ser 10:1021–1051
15. Li JX, Sanderson RD, Chai GY (2006) Sens Actuator B 114:182–191
16. Yin J, Coutris N, Huang Y (2010) Langmuir 26:16991–16999
17. Schacher F, Rudolph T, Wieberger F, Ulbricht M, Mller AHE (2009) ACS Appl Mater Interfac 1:1492–1503
18. Xu XC, Li JX, Li HS, Cao YH, He BQ, Zhang YZ (2009) J Membr Sci 326:103–110
19. Mairal AP, Greenberg AR, Krants WB, Bond LJ (1999) J Membr Sci 159:185–196
20. Feng X, Guo YF, Zhao YP, Li JX, Chen X, He XL, Chen L (2011) Chem J Chin U 32:1424–1430
21. Zuo DY, Zhu BK, Cao JH, Xu YY (2006) Chin J Polym Sci 24:281–289
22. Ying L, Kang ET, Neoh KG (2003) J Membr Sci 224:93–106
23. Wang WC, Tian XD, Feng YP, Cao B, Yang WT, Zhang LQ (2010) Ind Eng Chem Res 49:1684–1690
24. Yu Q, Zhang YX, Chen H, Zhou F, Wu ZQ, Huang H, Brash JL (2010) Langmuir 10:1021–1027
25. Ying L, Wang P, Kang ET, Neoh KG (2002) Macromolecules 35:673–679
26. Ying L, Yu WH, Kang ET, Neoh KG (2004) Langmuir 20:6032–6040
27. Xue J, Chen L, Wang HL, Zhang ZB, Zhu XL, Kang ET, Neoh KG (2008) Langmuir 24:14151–14158